
SMEFT combinations of Higgs measurements in ATLAS

Ana Cueto (UAM/CIAFF)

Effective Field Theories in Multiboson Production, Padua, June 2024



MINISTERIO
DE CIENCIA, INNOVACIÓN
Y UNIVERSIDADES



Financiado por
la Unión Europea
NextGenerationEU

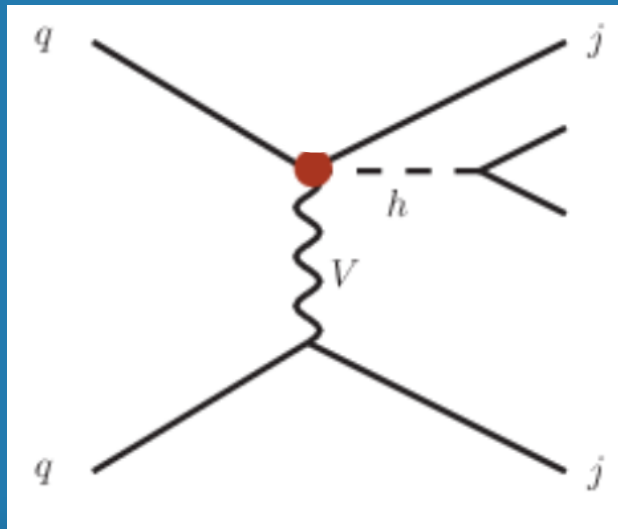


Plan de Recuperación,
Transformación y
Resiliencia

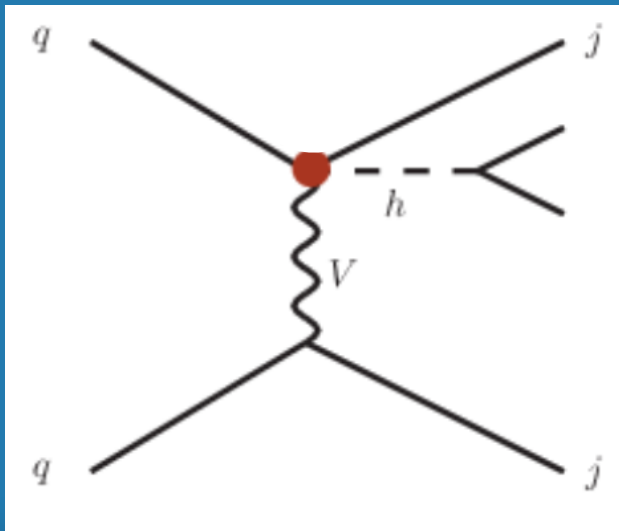


AGENCIA
ESTATAL DE
INVESTIGACIÓN

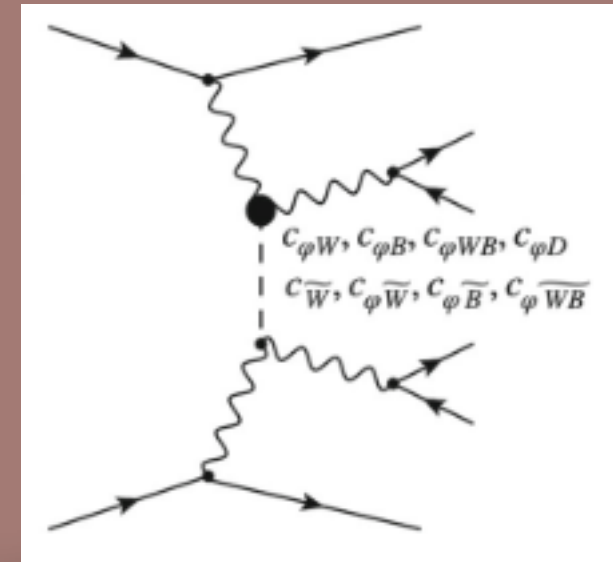
INTERPRETATIONS
OF HIGGS
COMBINATIONS:
HIGG-2022-17



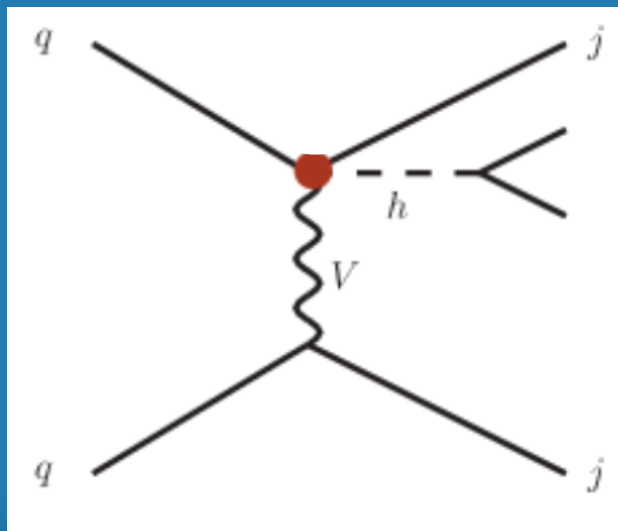
INTERPRETATIONS
OF HIGGS
COMBINATIONS:
HIGG-2022-17



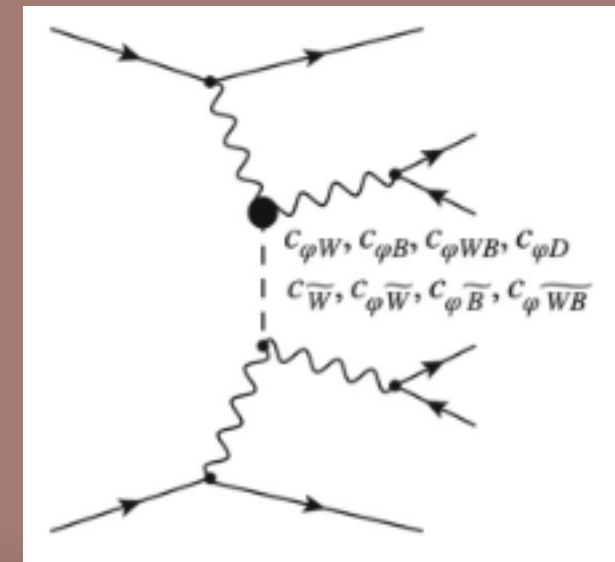
COMBINED EFT OF
HIGGS, WEAK BOSONS
AND EW PRECISION
DATA
ATL-PHYS-PUB-2022-037



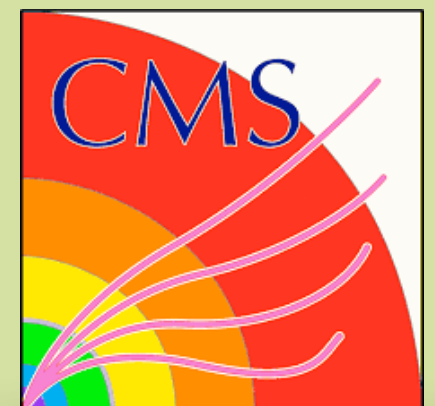
INTERPRETATIONS
OF HIGGS
COMBINATIONS:
HIGG-2022-17



COMBINED EFT OF
HIGGS, WEAK BOSONS
AND EW PRECISION
DATA
ATL-PHYS-PUB-2022-037

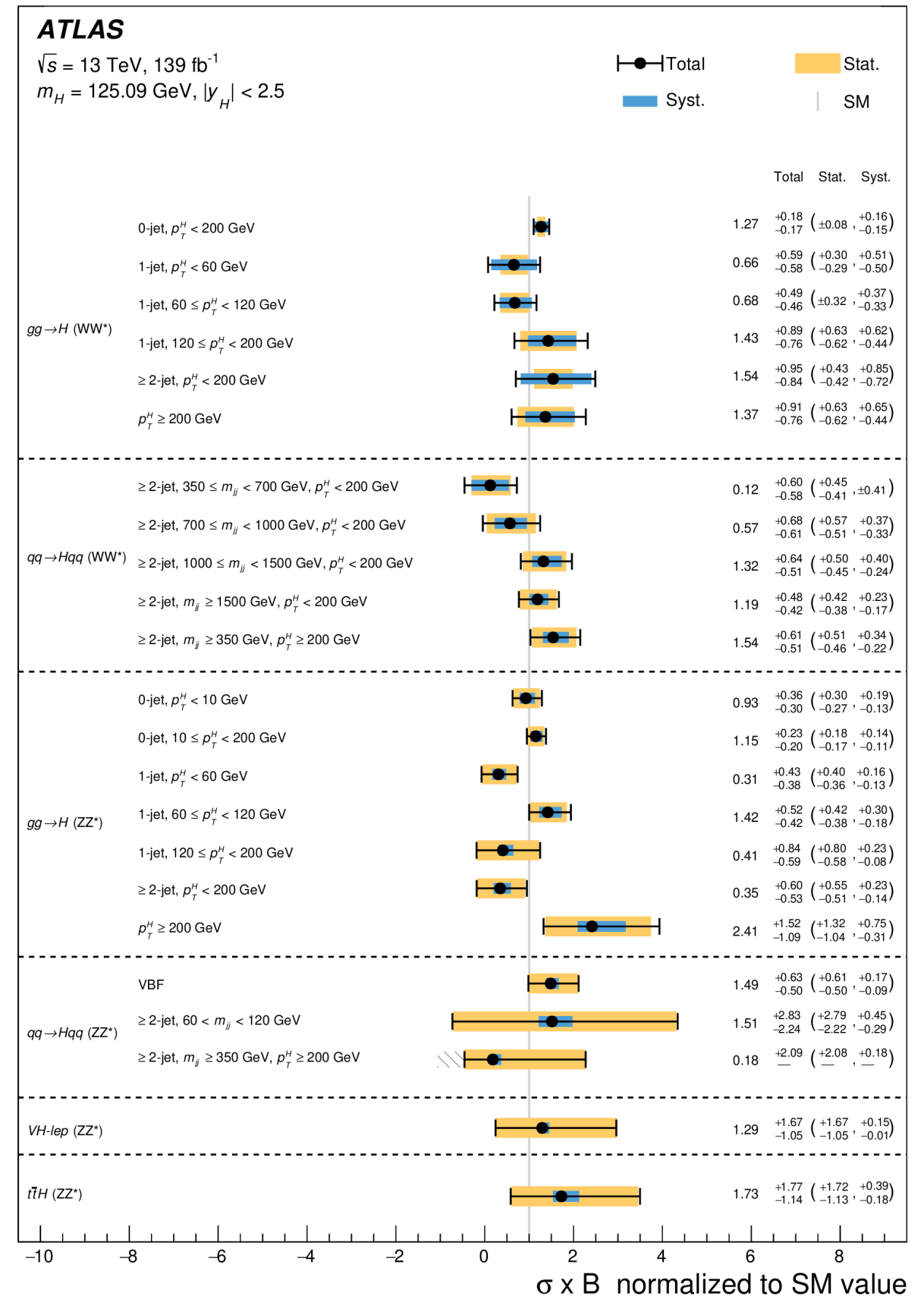


PARAMETRIZATIONS: ATLAS VS. CMS
(A LHC HIGGS WG 2 EXERCISE)



Simplified template cross sections

- Higgs couplings measurements performed in mutually exclusive kinematic bins in the different Higgs productions modes
- Not a fiducial measurement
→ Full phase-space folded into the measurement
- Does not include decay information
→ Suitable for combinations
- Definitions in a dedicated Rivet routine



Decay selection effects

- SMEFT-simulations only at particle level.

$$s_k^{\text{STXS}}(\mu_k, \theta) = \mathcal{L} \times \sum_{i,k',X} \mu_k^{i,k',X} \times (\sigma \times \mathcal{B})_{\text{SM,(N(N))NLO}}^{i,k',X}(\theta) \times \epsilon_{\text{STXS},k}^{i,k',X}(\theta)$$

Expected number of signal events

Signal strength, POI. This is changed by extracted parametrisation

Best XS value

Acceptance * Efficiency

Decay selection effects

- SMEFT-simulations only at particle level.

$$s_k^{\text{STXS}}(\mu_k, \theta) = \mathcal{L} \times \sum_{i,k',X} \mu_k^{i,k',X} \times (\sigma \times \mathcal{B})_{\text{SM,(N(N))NLO}}^{i,k',X}(\theta) \times \epsilon_{\text{STXS},k}^{i,k',X}(\theta)$$

Expected number of signal events

Signal strength, POI. This is changed by extracted parametrisation

Best XS value

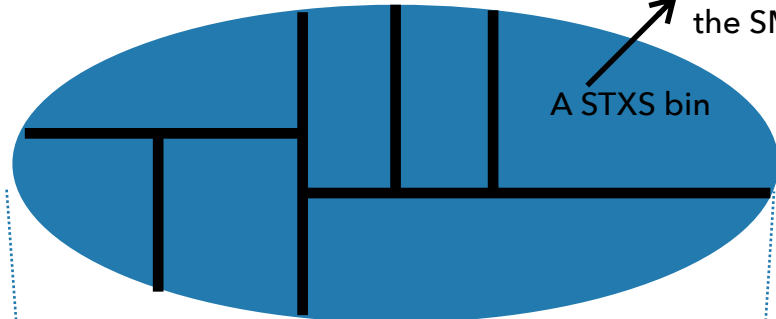
Acceptance * Efficiency

Particle level

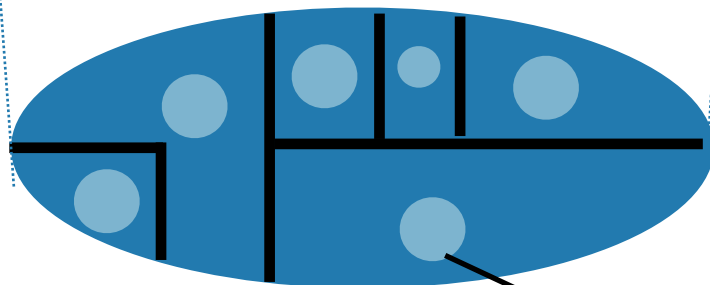
The phase-space of a given production mode

We consider changes of the SMEFT at this level

A STXS bin



Shrinks due to object selection, but assumed to be close enough to particle level. Events can migrate from a give region



Reconstruction level

Accessed region due to selection in decay

Decay selection effects

- SMEFT-simulations only at particle level.

$$s_k^{\text{STXS}}(\mu_k, \theta) = \mathcal{L} \times \sum_{i,k',X} \mu_k^{i,k',X} \times (\sigma \times \mathcal{B})_{\text{SM},(\text{N(N)})\text{NLO}}^{i,k',X}(\theta) \times \epsilon_{\text{STXS},k}^{i,k',X}(\theta)$$

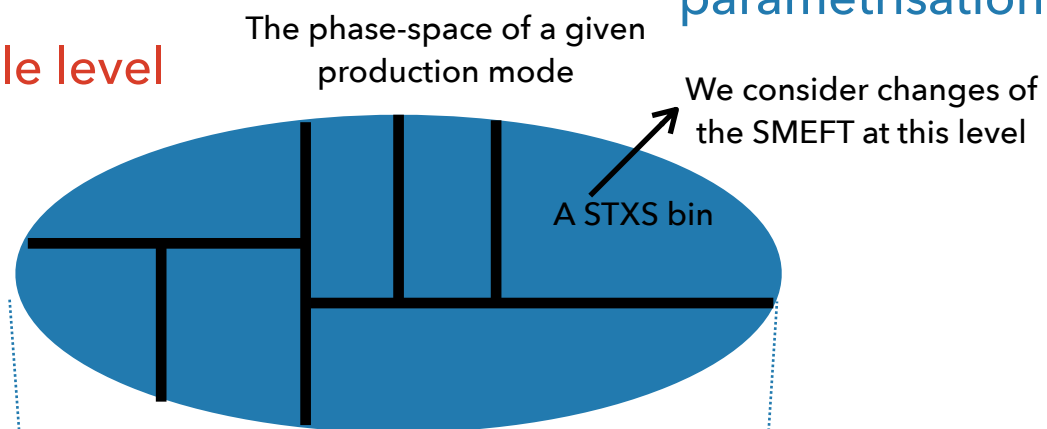
Expected number of signal events

Signal strength, POI. This is changed by extracted parametrisation

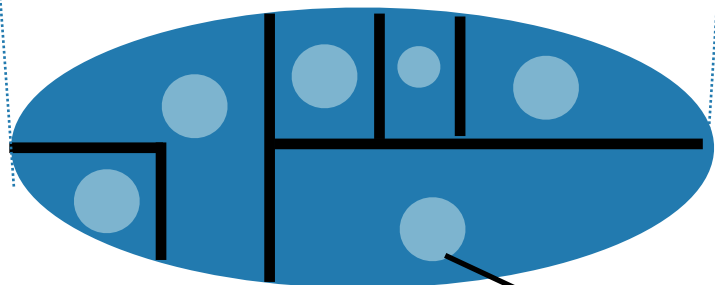
Best XS value

Acceptance * Efficiency

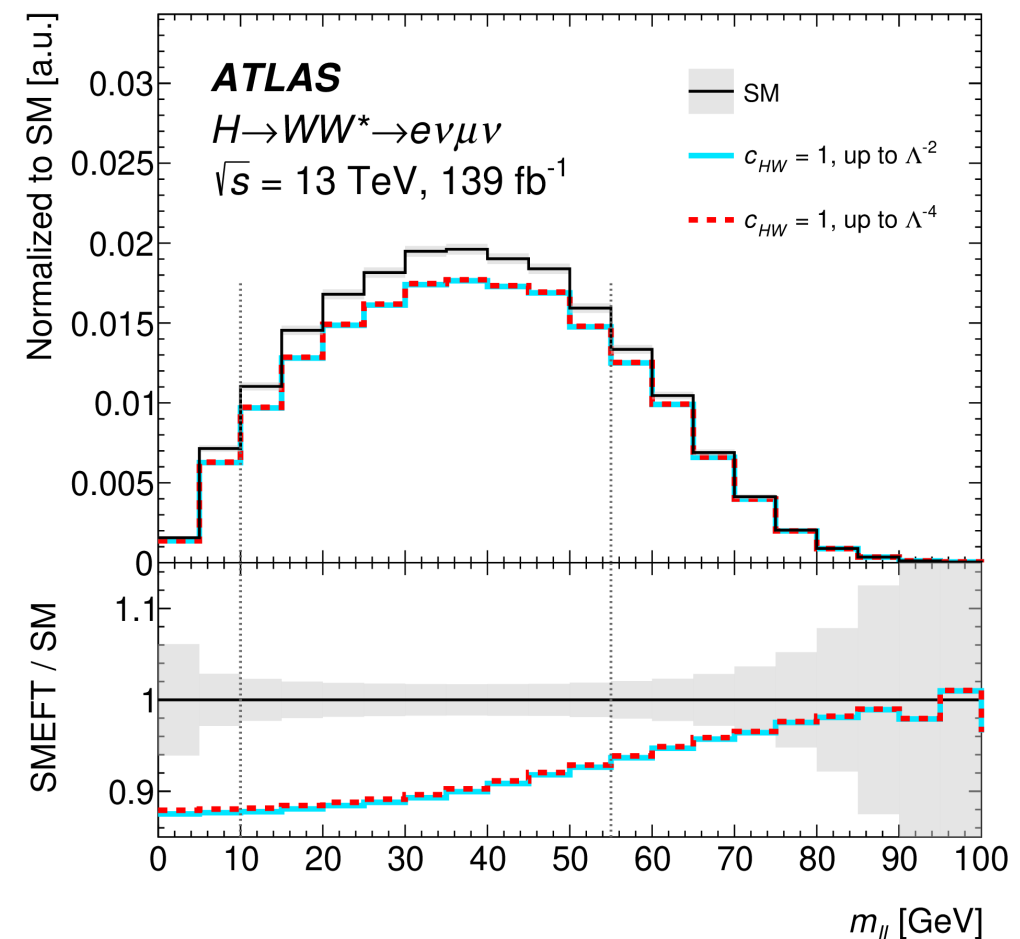
Particle level



Shrinks due to object selection, but assumed to be close enough to particle level. Events can migrate from a give region



Reconstruction level

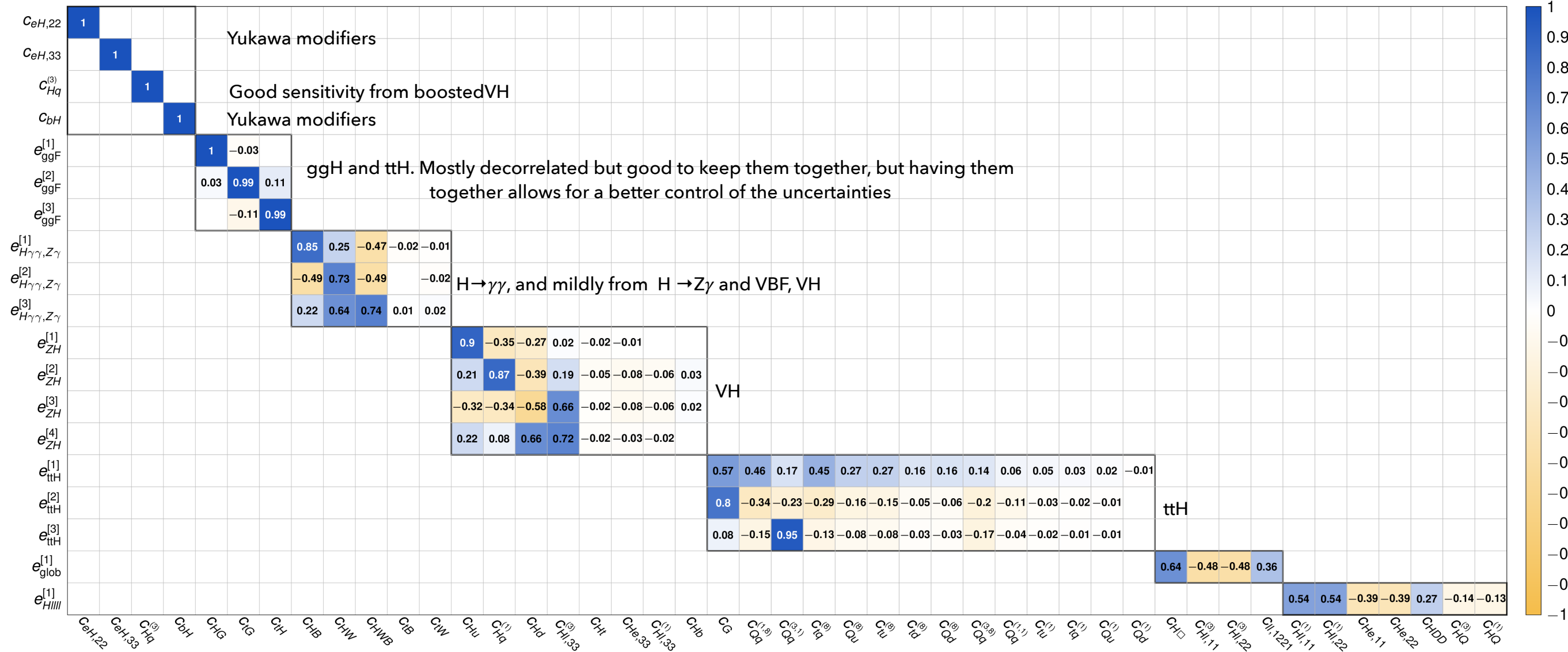


- Effects considered for $H \rightarrow ZZ^*/WW^*$ decays

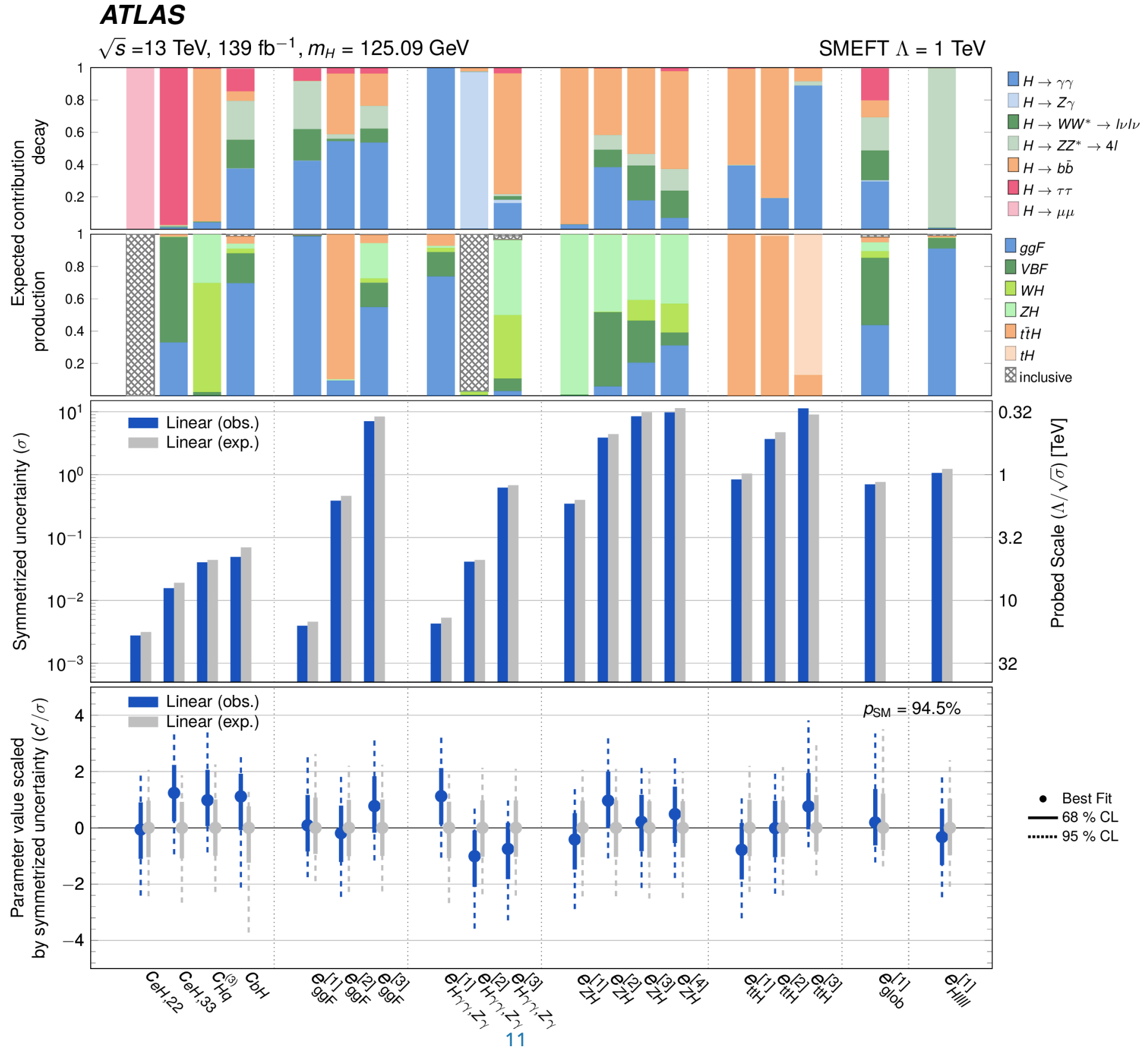
Phase-space rotation

- The goal is to perform a simultaneous analysis constraining all the Wilson coefficients at a time
- Search for eigendirections of the fit that can be constrained from a PCA analysis
- To try to keep some intuition on the results, they are grouped according to their physics impact (as much as possible). 18 directions constrained

ATLAS $\sqrt{s} = 13 \text{ TeV}, 139 \text{ fb}^{-1}$



Results

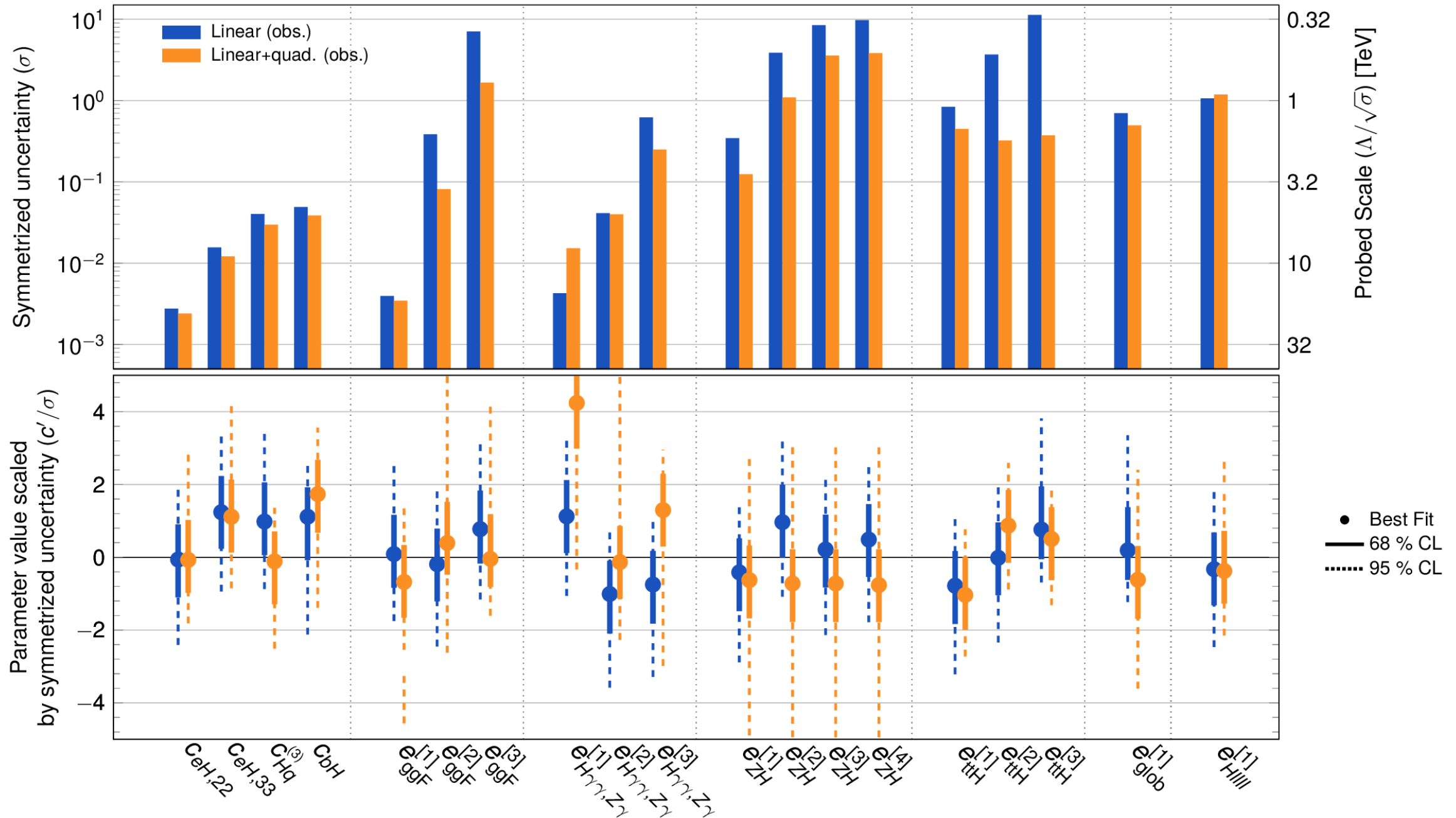


Results

ATLAS

$\sqrt{s} = 13 \text{ TeV}$, 139 fb^{-1} , $m_H = 125.09 \text{ GeV}$

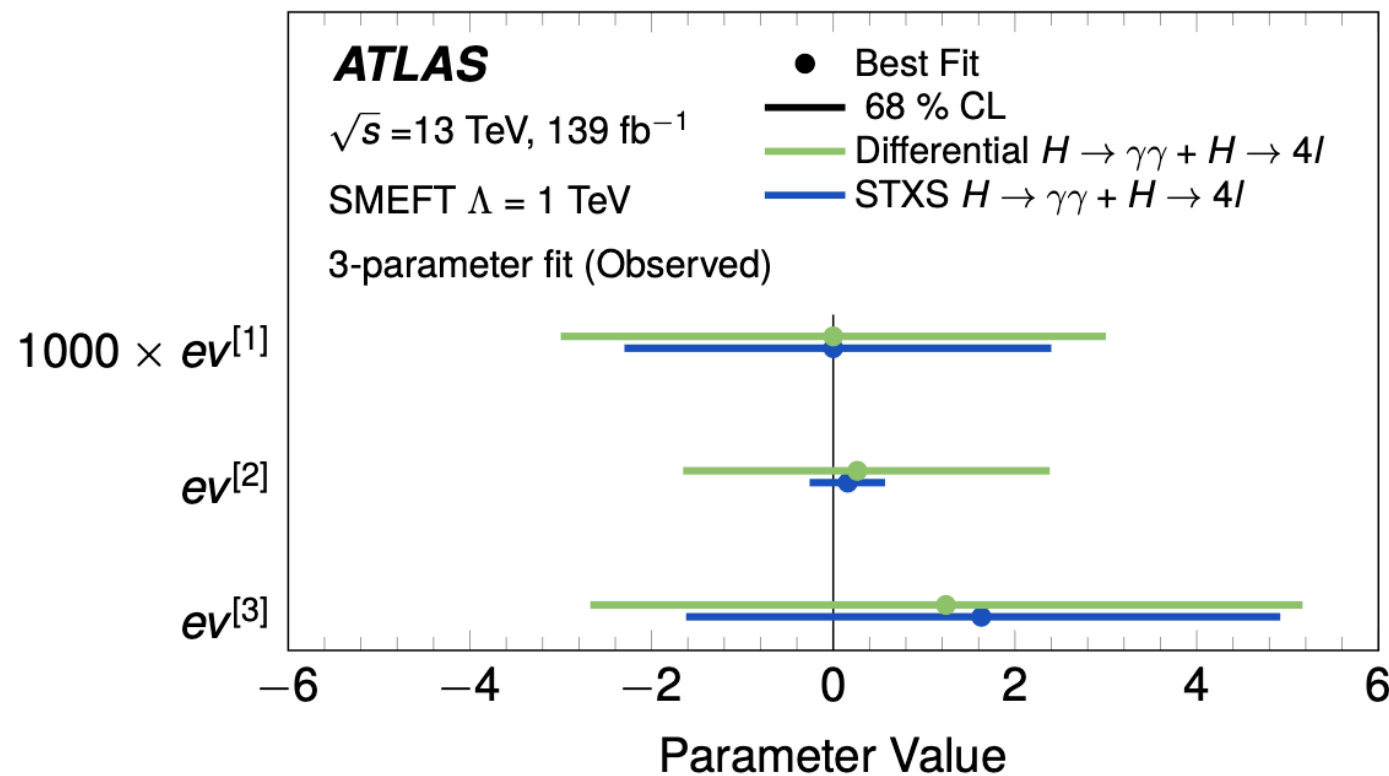
SMEFT $\Lambda = 1 \text{ TeV}$



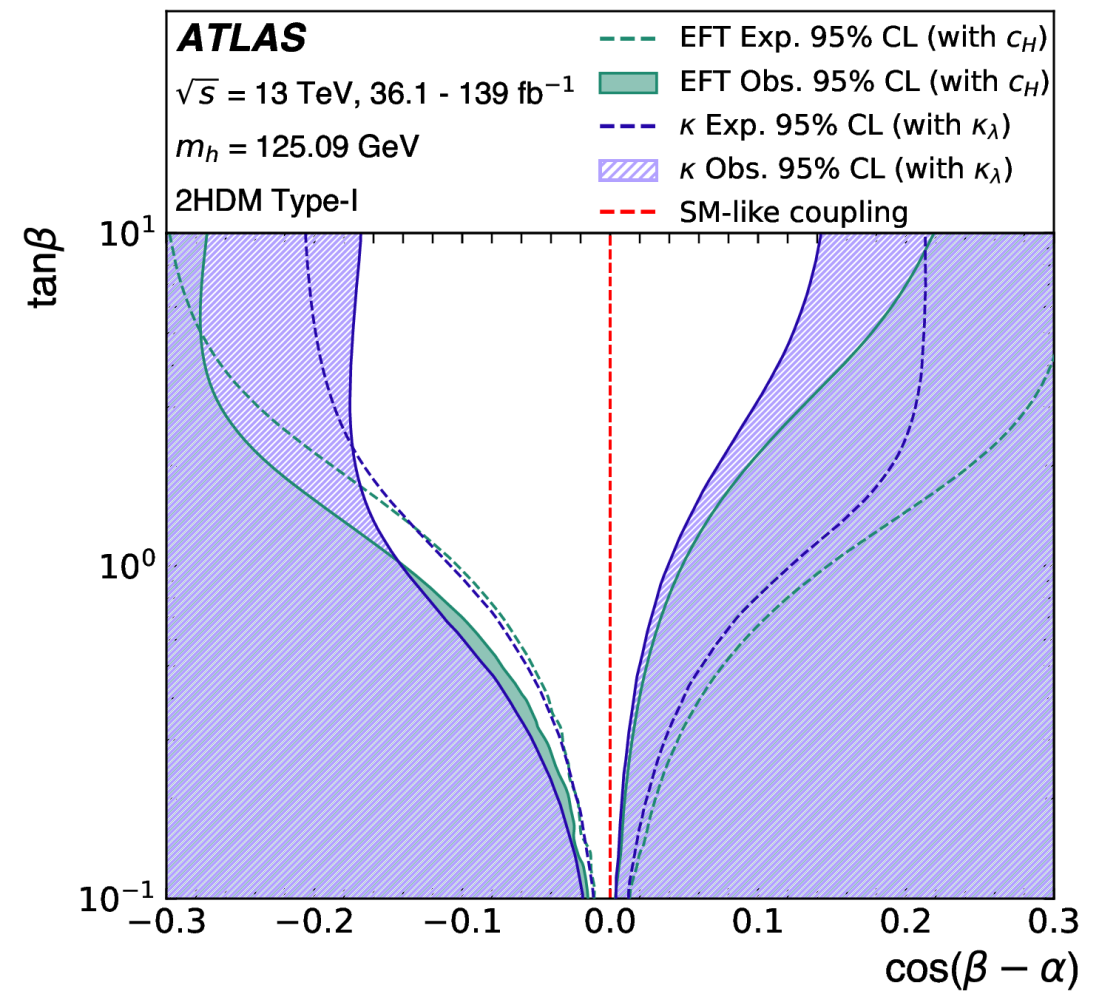
- All correlation matrices and profiled-likelihood scans in [HIGG-2022-17](#)
- Results extracted from a reparametrization of the combined likelihood, but also compared to simplified methodologies (see backup)

Other interpretations

- STXS interpretations shown here to see the interplay of a big sample of measurements
- Differential cross section measurements where also interpreted in terms of SMEFT. And 2HDM model constraint following a κ or EFT approach



$$\begin{aligned}
 ev^{[1]} &= 0.999c_{HG} - 0.035c_{tG} - 0.003c_{tH}, \\
 ev^{[2]} &= 0.035c_{HG} + 0.978c_{tG} + 0.205c_{tH}, \\
 ev^{[3]} &= -0.005c_{HG} - 0.205c_{tG} + 0.979c_{tH}.
 \end{aligned}$$



$$\frac{v^2 c_{iH}}{\Lambda^2} = -Y_i \eta_i \frac{\cos(\beta - \alpha)}{\tan \beta}$$

Electroweak inputs

- Differential cross section measurements of VV and VBF V processes:

Process	Important phase space requirements	Observable	\mathcal{L} [fb ⁻¹]	Ref.
$pp \rightarrow e^\pm \nu \mu^\mp \nu$	$m_{\ell\ell} > 55 \text{ GeV}, p_T^{\text{jet}} < 35 \text{ GeV}$	$p_T^{\text{lead. lep.}}$	36	[19]
$pp \rightarrow \ell^\pm \nu \ell^+ \ell^-$	$m_{\ell\ell} \in (81, 101) \text{ GeV}$	m_T^{WZ}	36	[20]
$pp \rightarrow \ell^+ \ell^- \ell^+ \ell^-$	$m_{4\ell} > 180 \text{ GeV}$	m_{Z2}	139	[21]
$pp \rightarrow \ell^+ \ell^- jj$	$m_{jj} > 1000 \text{ GeV}, m_{\ell\ell} \in (81, 101) \text{ GeV}$	$\Delta\phi_{jj}$	139	[22]

Electroweak inputs

- Differential cross section measurements of VV and VBF V processes:

Process	Important phase space requirements	Observable	\mathcal{L} [fb^{-1}]	Ref.
$pp \rightarrow e^\pm \nu \mu^\mp \nu$	$m_{\ell\ell} > 55 \text{ GeV}, p_{\text{T}}^{\text{jet}} < 35 \text{ GeV}$	$p_{\text{T}}^{\text{lead. lep.}}$	36	[19]
$pp \rightarrow \ell^\pm \nu \ell^+ \ell^-$	$m_{\ell\ell} \in (81, 101) \text{ GeV}$	m_{T}^{WZ}	36	[20]
$pp \rightarrow \ell^+ \ell^- \ell^+ \ell^-$	$m_{4\ell} > 180 \text{ GeV}$	m_{Z2}	139	[21]
$pp \rightarrow \ell^+ \ell^- jj$	$m_{jj} > 1000 \text{ GeV}, m_{\ell\ell} \in (81, 101) \text{ GeV}$	$\Delta\phi_{jj}$	139	[22]

Observable	Measurement	Prediction	Ratio
Γ_Z [MeV]	2495.2 ± 2.3	2495.7 ± 1	0.9998 ± 0.0010
R_ℓ^0	20.767 ± 0.025	20.758 ± 0.008	1.0004 ± 0.0013
R_c^0	0.1721 ± 0.0030	0.17223 ± 0.00003	0.999 ± 0.017
R_b^0	0.21629 ± 0.00066	0.21586 ± 0.00003	1.0020 ± 0.0031
$A_{\text{FB}}^{0,\ell}$	0.0171 ± 0.0010	0.01718 ± 0.00037	0.995 ± 0.062
$A_{\text{FB}}^{0,c}$	0.0707 ± 0.0035	0.0758 ± 0.0012	0.932 ± 0.048
$A_{\text{FB}}^{0,b}$	0.0992 ± 0.0016	0.1062 ± 0.0016	0.935 ± 0.021
σ_{had}^0 [pb]	41488 ± 6	41489 ± 5	0.99998 ± 0.00019

- 8 precision observables from LEP+SLC

Electroweak inputs

- Differential cross section measurements of VV and VBF V processes:

Process	Important phase space requirements	Observable	\mathcal{L} [fb ⁻¹]	Ref.
$pp \rightarrow e^\pm \nu \mu^\mp \nu$	$m_{\ell\ell} > 55 \text{ GeV}, p_T^{\text{jet}} < 35 \text{ GeV}$	$p_T^{\text{lead. lep.}}$	36	[19]
$pp \rightarrow \ell^\pm \nu \ell^+ \ell^-$	$m_{\ell\ell} \in (81, 101) \text{ GeV}$	m_T^{WZ}	36	[20]
$pp \rightarrow \ell^+ \ell^- \ell^+ \ell^-$	$m_{4\ell} > 180 \text{ GeV}$	m_{Z2}	139	[21]
$pp \rightarrow \ell^+ \ell^- jj$	$m_{jj} > 1000 \text{ GeV}, m_{\ell\ell} \in (81, 101) \text{ GeV}$	$\Delta\phi_{jj}$	139	[22]

Observable	Measurement	Prediction	Ratio
Γ_Z [MeV]	2495.2 ± 2.3	2495.7 ± 1	0.9998 ± 0.0010
R_ℓ^0	20.767 ± 0.025	20.758 ± 0.008	1.0004 ± 0.0013
R_c^0	0.1721 ± 0.0030	0.17223 ± 0.00003	0.999 ± 0.017
R_b^0	0.21629 ± 0.00066	0.21586 ± 0.00003	1.0020 ± 0.0031
$A_{\text{FB}}^{0,\ell}$	0.0171 ± 0.0010	0.01718 ± 0.00037	0.995 ± 0.062
$A_{\text{FB}}^{0,c}$	0.0707 ± 0.0035	0.0758 ± 0.0012	0.932 ± 0.048
$A_{\text{FB}}^{0,b}$	0.0992 ± 0.0016	0.1062 ± 0.0016	0.935 ± 0.021
σ_{had}^0 [pb]	41488 ± 6	41489 ± 5	0.99998 ± 0.00019

- 8 precision observables from LEP+SLC

- Similar inputs as in the Higgs combination, but updated results in some cases (e.g. $H \rightarrow \gamma\gamma$) or low-BR channels $H \rightarrow \mu\mu$ and $H \rightarrow Z\gamma$

Statistical combination

- Removed overlap regions: e.g off-shell region of the 4l analysis that overlaps with the $H \rightarrow 4l$ CR

- Common sources of systematic uncertainties treated as correlated between SMEW and Higgs measurements

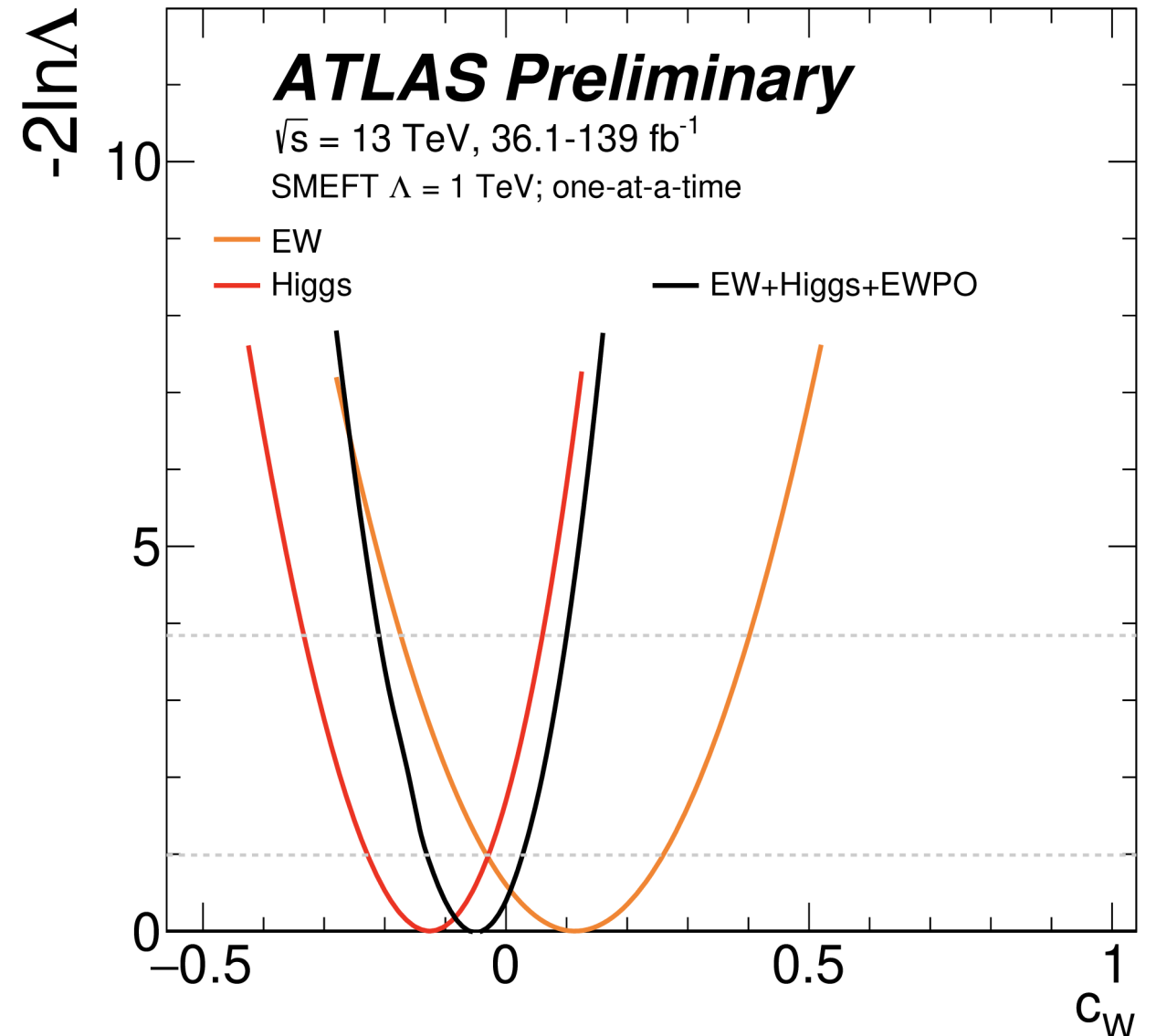
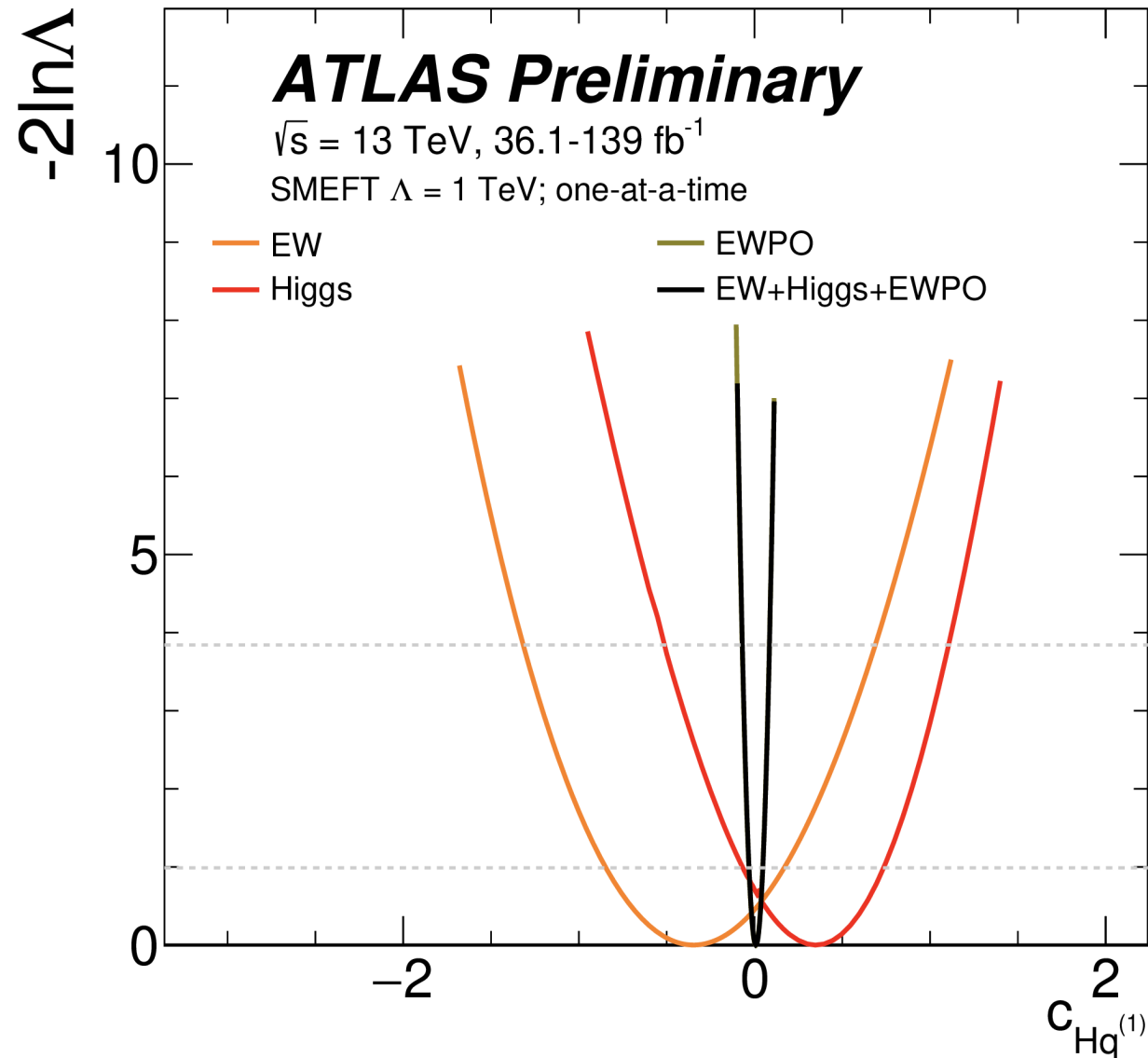
Source of correlated uncertainty	Parameters
Luminosity (common part 2015–2018)	1
Luminosity 2015/2016	1
Luminosity 2017/2018	1
Pile-up modelling	1
Pile-up jet suppression	1
Jet energy scale (pile-up modelling)	3
Jet energy scale η -inter-calibration	1
Jet energy resolution	12
WW modelling (WW and $H \rightarrow WW^*$)	2

- For EWPO, experimental and theory uncertainties in the covariance matrix

- Limits from a combined likelihood built as the product of the individual ones

Results: 1D scans

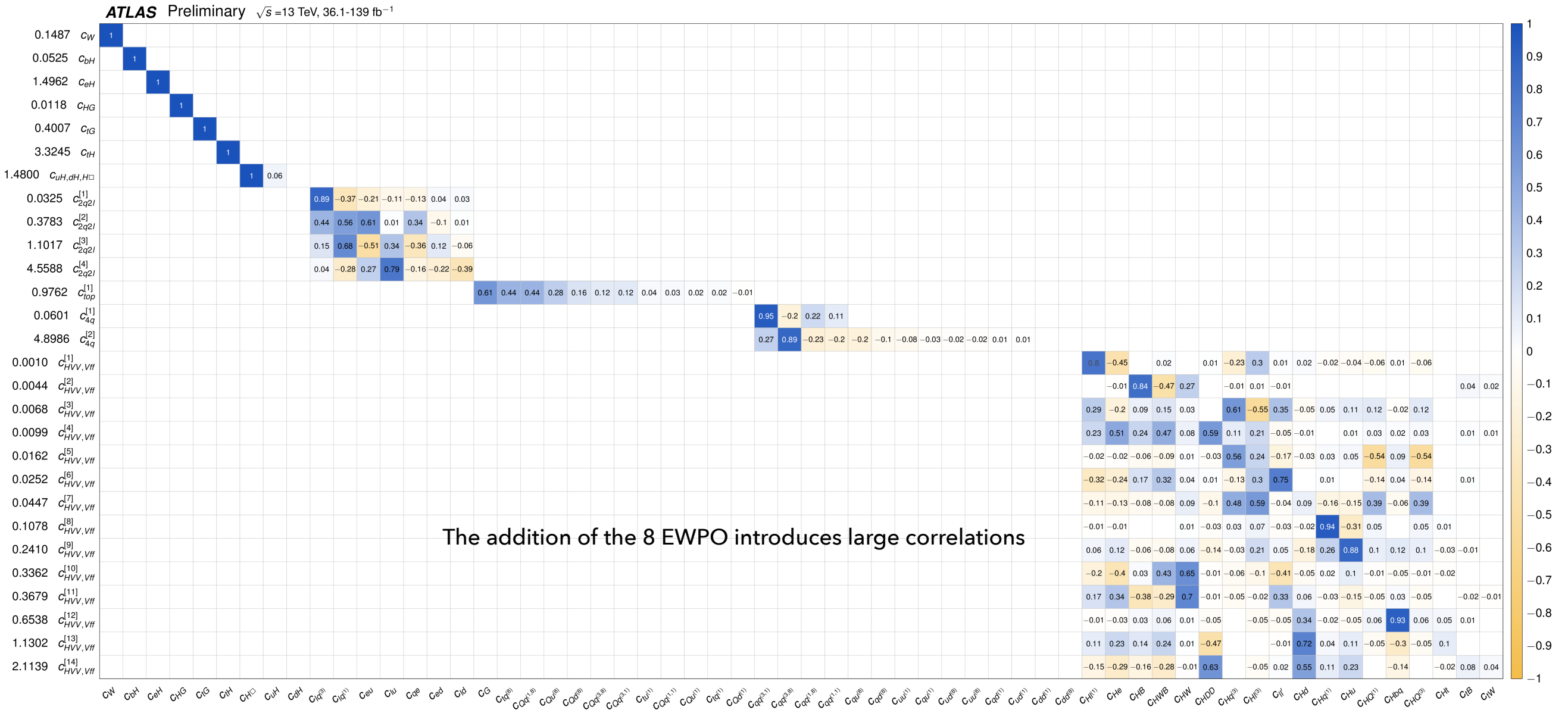
- 1D results give a good handle of the sensitivity of different measurements to a given operator



- Depends on the precision of the measurement and the impact of each Wilson coefficient on the measurement

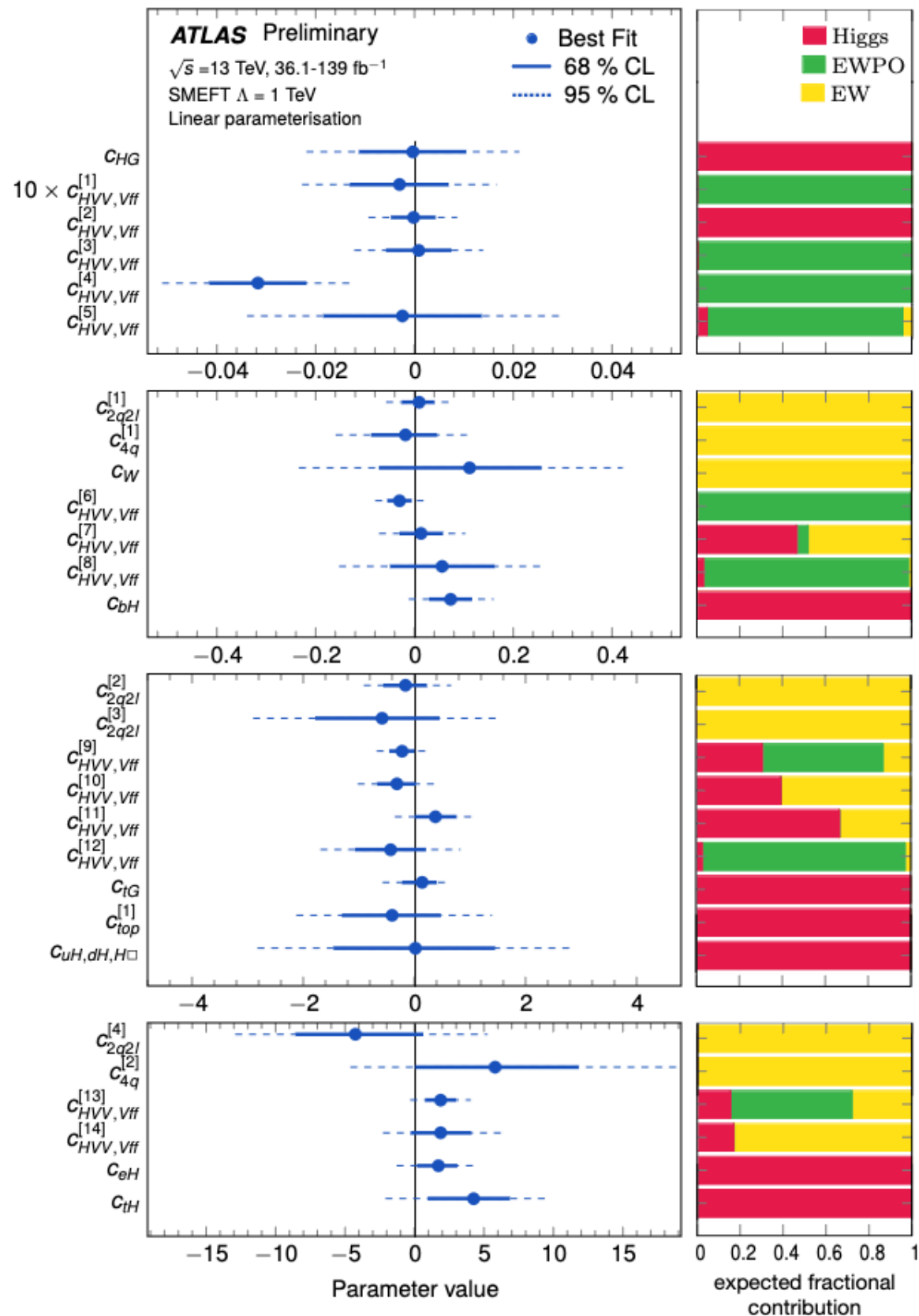
Results: simultaneous fits

- PCA components selects 28 directions



Only keeping those with $\sigma < 5$

Results: simultaneous fits



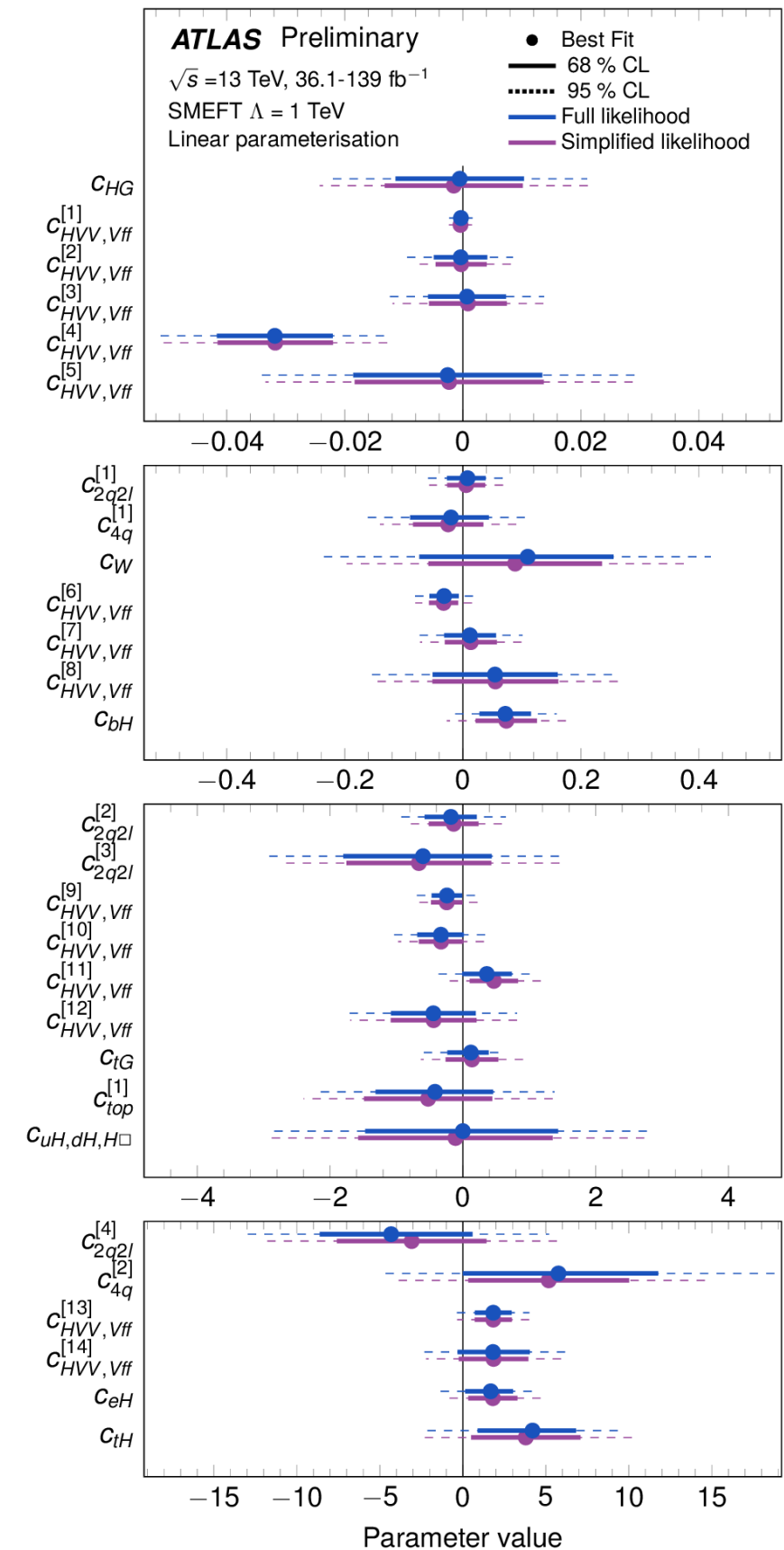
- Only linear parametrisation for EWPO
- Results also obtained for ATLAS only
- Contribution from a group I of measurement computed assuming Gaussian approximation

$$\frac{\sigma_i^{-2}}{\sum_j \sigma_j^{-2}}$$

- Some directions constraint from a single measurement, but others benefit from the combination

What experimentalist do/do not do well

- We have access to the full likelihoods and understand well the origin of systematic uncertainties.
 - ➔ Some analyses now making them public
 - ➔ Simplified Gaussian models usually perform well
- Specially in combinations, where several parametrisation need to be worked out, it is easy to overlook mistakes
 - ➔ Having benchmarks can greatly reduced these mistakes



LHC Higgs WG project

- Compare ATLAS and CMS parametrisations of single-Higgs production modes and decay channels
 - ➔ Provide a common format to publish parametrisation with all the needed information to reproduce the results
 - ➔ Provide a benchmark parametrisation for Higgs STXS
 - ➔ Provide the full toolchain based on MadGraph simulations with the EFT2Obs package maintained by CMS colleagues

LHC HIGGS WORKING GROUP*

PUBLIC NOTE

Publishing SMEFT parametrisations for HEP measurements: a proposal for a common data format and simulation toolchain for Higgs simplified template cross sections

LHC Higgs WG project

```
"metadata": {
  "coefficients": [ "chb", "chbox", "chd", "ct",
  "observable_shape": "(1,)",
  "observable_names": [ "example" ],
  "author": "Jane Bloggs",
  "contact": "j.bloggs@cern.ch",
  "date [DD/MM/YY]": "15/11/2023",
  "description": "An example SMEFT parametrisation",
  "documentation": [ "https://mydocumentation." ],
  "tool_version": "MG5_aMC_v2_X_Y",
  "basis": "warsaw",
  "flavor_scheme": "topU3L",
  "inputs": {
    "Lambda": 1000,
    "MW": 91.1876,
    "GF": 1.16638e-05,
    "aS": 0.1181,
    "MH": 125.0,
    "MB": 3.237,
    "MT": 173.2
  },
  "EW_input_scheme": "MW_MZ_GF",
  "EFT_order": "quadratic",
  "scale_choice": 125.09,
  "pertubative_order_QCD": "LO",
  "pertubative_order_QED/EW": "LO",
  "method": "reweighting"
},
"data": {
  "central": {
    "SM": [ 10.0 ],
    "a_chb": [ 1.0 ],
    ...
  }
}
```

Partial example of a JSON file

- Few things that the exercise has helped to notice
 - ➔ Wrong scale used by ATLAS for ggH (dynamical scale vs the correct fixed scale)
 - ➔ FS not consistently treated in ATLAS
 - ➔ CMS inherited typos in $H \rightarrow \gamma\gamma$ analytic results
 - ➔ Different treatment of ggZH between experiments (gg > hz vs gg > h l+ l-)

WORK IN PROGRESS

Summary

- ATLAS keeps its program to provide SMEFT interpretations of SM measurements in combinations
 - ➔ Higgs results based on STXS published, now also extended to differential cross sections
 - ➔ EW combinations exercised in combination with Higgs analyses
 - ➔ No public results from top, but active work in the area
 - ➔ Interest also in B-physics
- Final goal is to perform interpretations of combinations of measurements from the different sectors
- The LHC WGs play a very important role in the harmonisation across experiments (and ultimately also with theory interpretations)

The background of the image is a clear blue sky with scattered, wispy white clouds. The clouds are most prominent in the upper and lower portions of the frame, leaving a clear blue area in the center where the text is located.

Back-up

Parametrisation

- Different approaches in different publications. For linear parametrisation:

$$\begin{aligned}
 (\sigma \times \mathcal{B})_{\text{SMEFT}}^{i,k',H \rightarrow X} &= (\sigma \times \mathcal{B})_{\text{SM},((\text{N})\text{N})\text{NLO}}^{i,k',H \rightarrow X} \times \left(1 + \frac{\sigma_{\text{int},(\text{N})\text{LO}}^{i,k'}}{\sigma_{\text{SM},(\text{N})\text{LO}}^{i,k'}} \right) \times \left(\frac{1 + \frac{\Gamma_{\text{int}}^{H \rightarrow X}}{\Gamma_{\text{SM}}^{H \rightarrow X}}}{1 + \frac{\Gamma_{\text{int}}^H}{\Gamma_{\text{SM}}^H}} \right) \\
 &= (\sigma \times \mathcal{B})_{\text{SM},((\text{N})\text{N})\text{NLO}}^{i,k',H \rightarrow X} \times \left(1 + \sum_j A_j^{\sigma_{i,k'}} c_j \right) \times \left(\frac{1 + \sum_j A_j^{\Gamma_{H \rightarrow X}} c_j}{1 + \sum_j A_j^{\Gamma^H} c_j} \right), \\
 &= (\sigma \times \mathcal{B})_{\text{SM},((\text{N})\text{N})\text{NLO}}^{i,k',H \rightarrow X} \times \left(\frac{1 + \sum_j (A_j^{\sigma_{i,k'}} + A_j^{\Gamma_{H \rightarrow X}}) c_j + \mathcal{O}(\Lambda^{-4})}{1 + \sum_j A_j^{\Gamma^H} c_j + \mathcal{O}(\Lambda^{-4})} \right),
 \end{aligned}$$

No Taylor expansion of the total width. This is important for operators that are poorly constrained and can take up large values.

- For quadratic:

$$\begin{aligned}
 (\sigma \times \mathcal{B})_{\text{SMEFT}}^{i,k',H \rightarrow X} &= (\sigma \times \mathcal{B})_{\text{SM},((\text{N})\text{N})\text{NLO}}^{i,k',H \rightarrow X} \left(1 + \sum_j A_j^{\sigma_{i,k'}} c_j + \sum_{j,l \geq j} B_{jl}^{\sigma_{i,k'}} c_j c_l \right) \left(\frac{1 + \sum_j A_j^{\Gamma_{H \rightarrow X}} c_j + \sum_{j,l \geq j} B_{jl}^{\Gamma_{H \rightarrow X}} c_j c_l}{1 + \sum_j A_j^{\Gamma^H} c_j + \sum_{j,l \geq j} B_{jl}^{\Gamma^H} c_j c_l} \right), \\
 &= (\sigma \times \mathcal{B})_{\text{SM},((\text{N})\text{N})\text{NLO}}^{i,k',H \rightarrow X} \cdot \\
 &\quad \left(\frac{1 + \sum_j (A_j^{\sigma_{i,k'}} + A_j^{\Gamma_{H \rightarrow X}}) c_j + \sum_{j,l} (A_j^{\sigma_{i,k'}} A_l^{\Gamma_{H \rightarrow X}}) c_j c_l + \sum_{j,l \geq j} (B_{jl}^{\sigma_{i,k'}} + B_{jl}^{\Gamma_{H \rightarrow X}}) c_j c_l + \mathcal{O}(\Lambda^{-6})}{1 + \sum_j (A_j^{\Gamma^H}) c_j + \sum_{j,l \geq j} (B_{jl}^{\Gamma^H}) c_j c_l + \mathcal{O}(\Lambda^{-6})} \right) \quad (13)
 \end{aligned}$$

Numerator and denominator are second-order polynomials, but the denominator is not further expanded

Operators

Wilson coefficient	Operator	Wilson coefficient	Operator
c_H	$(H^\dagger H)^3$	$c_{Qq}^{(1,1)}$	$(\bar{Q}\gamma_\mu Q)(\bar{q}\gamma^\mu q)$
$c_{H\Box}$	$(H^\dagger H)\Box(H^\dagger H)$	$c_{Qq}^{(1,8)}$	$(\bar{Q}T^a\gamma_\mu Q)(\bar{q}T^a\gamma^\mu q)$
c_G	$f^{abc}G_\mu^{av}G_\nu^{bp}G_\rho^{c\mu}$	$c_{Qq}^{(3,1)}$	$(\bar{Q}\sigma^i\gamma_\mu Q)(\bar{q}\sigma^i\gamma^\mu q)$
c_W	$\epsilon^{IJK}W_\mu^{I\nu}W_\nu^{J\rho}W_\rho^{K\mu}$	$c_{Qq}^{(3,8)}$	$(\bar{Q}\sigma^iT^a\gamma_\mu Q)(\bar{q}\sigma^iT^a\gamma^\mu q)$
c_{HDD}	$(H^\dagger D^\mu H)^*(H^\dagger D_\mu H)$	$c_{qq}^{(3,1)}$	$(\bar{q}\sigma^i\gamma_\mu q)(\bar{q}\sigma^i\gamma^\mu q)$
c_{HG}	$H^\dagger H G_{\mu\nu}^A G^{A\mu\nu}$	$c_{tu}^{(1)}$	$(\bar{t}\gamma_\mu t)(\bar{u}\gamma^\mu u)$
c_{HB}	$H^\dagger H B_{\mu\nu} B^{\mu\nu}$	$c_{tu}^{(8)}$	$(\bar{t}T^a\gamma_\mu t)(\bar{u}T^a\gamma^\mu u)$
c_{HW}	$H^\dagger H W_{\mu\nu}^I W^{I\mu\nu}$	$c_{td}^{(1)}$	$(\bar{t}\gamma_\mu t)(\bar{d}\gamma^\mu d)$
c_{HWB}	$H^\dagger \tau^I H W_{\mu\nu}^I B^{\mu\nu}$	$c_{td}^{(8)}$	$(\bar{t}T^a\gamma_\mu t)(\bar{d}T^a\gamma^\mu d)$
$c_{HL,11}^{(1)}$	$(H^\dagger i \overleftrightarrow{D}_\mu H)(\bar{l}_1\gamma^\mu l_1)$	$c_{Qu}^{(1)}$	$(\bar{Q}\gamma_\mu Q)(\bar{u}\gamma^\mu u)$
$c_{HL,22}^{(1)}$	$(H^\dagger i \overleftrightarrow{D}_\mu H)(\bar{l}_2\gamma^\mu l_2)$	$c_{Qu}^{(8)}$	$(\bar{Q}T^a\gamma_\mu Q)(\bar{u}T^a\gamma^\mu u)$
$c_{HL,33}^{(1)}$	$(H^\dagger i \overleftrightarrow{D}_\mu H)(\bar{l}_3\gamma^\mu l_3)$	$c_{Qd}^{(1)}$	$(\bar{Q}\gamma_\mu Q)(\bar{d}\gamma^\mu d)$
$c_{HL,11}^{(3)}$	$(H^\dagger i \overleftrightarrow{D}_\mu^I H)(\bar{l}_1\tau^I\gamma^\mu l_1)$	$c_{Qd}^{(8)}$	$(\bar{Q}T^a\gamma_\mu Q)(\bar{d}T^a\gamma^\mu d)$
$c_{HL,22}^{(3)}$	$(H^\dagger i \overleftrightarrow{D}_\mu^I H)(\bar{l}_2\tau^I\gamma^\mu l_2)$	$c_{tq}^{(1)}$	$(\bar{q}\gamma_\mu q)(\bar{t}\gamma^\mu t)$
$c_{HL,33}^{(3)}$	$(H^\dagger i \overleftrightarrow{D}_\mu^I H)(\bar{l}_3\tau^I\gamma^\mu l_3)$	$c_{tq}^{(8)}$	$(\bar{q}T^a\gamma_\mu q)(\bar{t}T^a\gamma^\mu t)$
$c_{He,11}$	$(H^\dagger i \overleftrightarrow{D}_\mu H)(\bar{e}_1\gamma^\mu e_1)$	$c_{eH,22}$	$(H^\dagger H)(\bar{l}_2 e_2 H)$
$c_{He,22}$	$(H^\dagger i \overleftrightarrow{D}_\mu H)(\bar{e}_2\gamma^\mu e_2)$	$c_{eH,33}$	$(H^\dagger H)(\bar{l}_3 e_3 H)$
$c_{He,33}$	$(H^\dagger i \overleftrightarrow{D}_\mu H)(\bar{e}_3\gamma^\mu e_3)$	c_{uH}	$(H^\dagger H)(\bar{q}Y_u^\dagger u \tilde{H})$
$c_{Hq}^{(1)}$	$(H^\dagger i \overleftrightarrow{D}_\mu H)(\bar{q}\gamma^\mu q)$	c_{tH}	$(H^\dagger H)(\bar{Q}\tilde{H}t)$
$c_{Hq}^{(3)}$	$(H^\dagger i \overleftrightarrow{D}_\mu^I H)(\bar{q}\tau^I\gamma^\mu q)$	c_{bH}	$(H^\dagger H)(\bar{Q}Hb)$
c_{Hu}	$(H^\dagger i \overleftrightarrow{D}_\mu H)(\bar{u}_p\gamma^\mu u_r)$	c_{tG}	$(\bar{Q}\sigma^{\mu\nu}T^A t)\tilde{H}G_{\mu\nu}^A$
c_{Hd}	$(H^\dagger i \overleftrightarrow{D}_\mu H)(\bar{d}_p\gamma^\mu d_r)$	c_{tW}	$(\bar{Q}\sigma^{\mu\nu}t)\tau^I\tilde{H}W_{\mu\nu}^I$
$c_{HQ}^{(1)}$	$(H^\dagger i \overleftrightarrow{D}_\mu H)(\bar{Q}\gamma^\mu Q)$	c_{tB}	$(\bar{Q}\sigma^{\mu\nu}t)\tilde{H}B_{\mu\nu}$
$c_{HQ}^{(3)}$	$(H^\dagger i \overleftrightarrow{D}_\mu^I H)(\bar{Q}\tau^I\gamma^\mu Q)$	$c_{ll,1221}$	$(\bar{l}_1\gamma_\mu l_2)(\bar{l}_2\gamma^\mu l_1)$
c_{Ht}	$(H^\dagger i \overleftrightarrow{D}_\mu H)(\bar{t}\gamma^\mu t)$		
c_{Hb}	$(H^\dagger i \overleftrightarrow{D}_\mu H)(\bar{b}\gamma^\mu b)$		

Uncertainties

- Parameter uncertainties sources

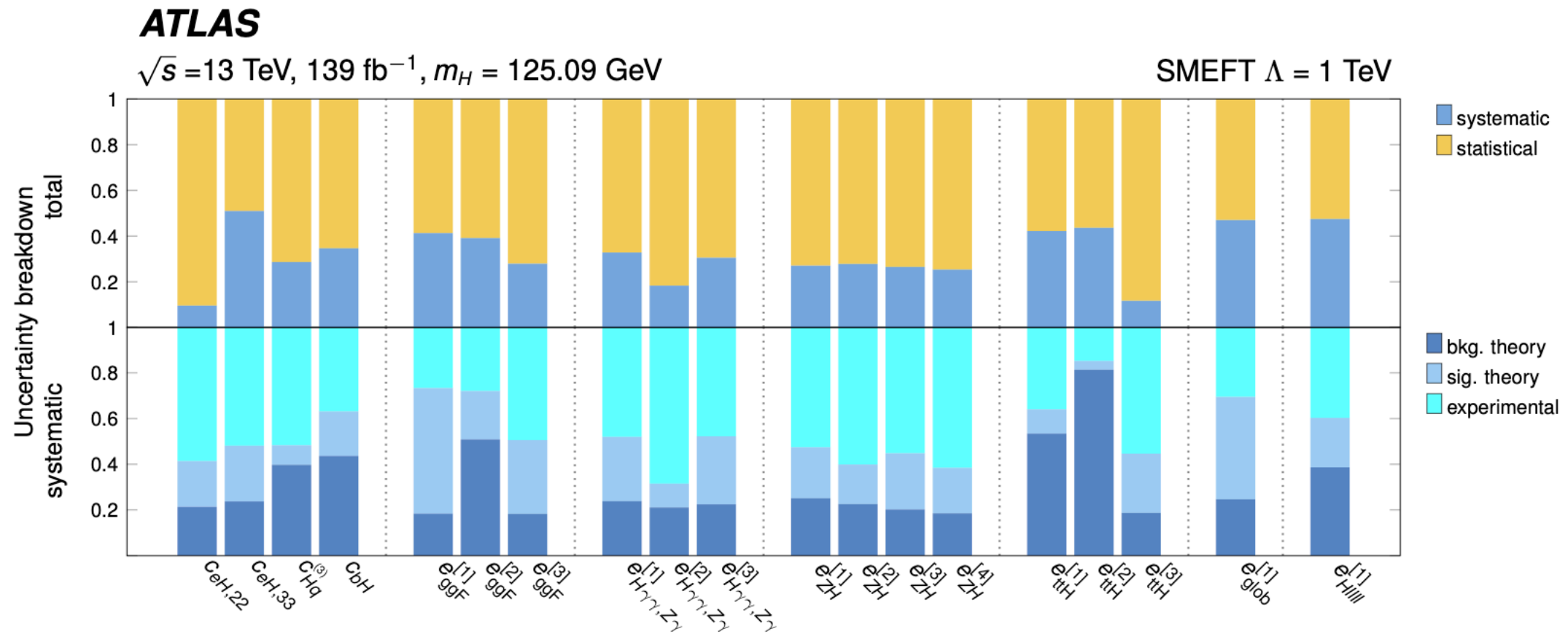
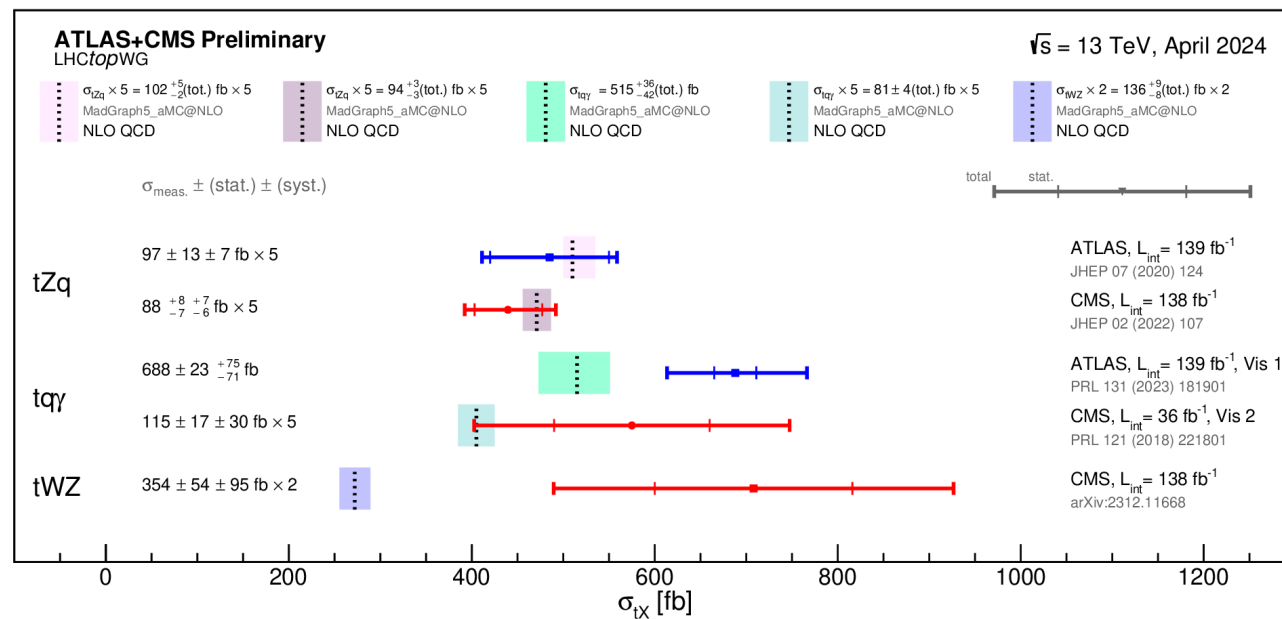
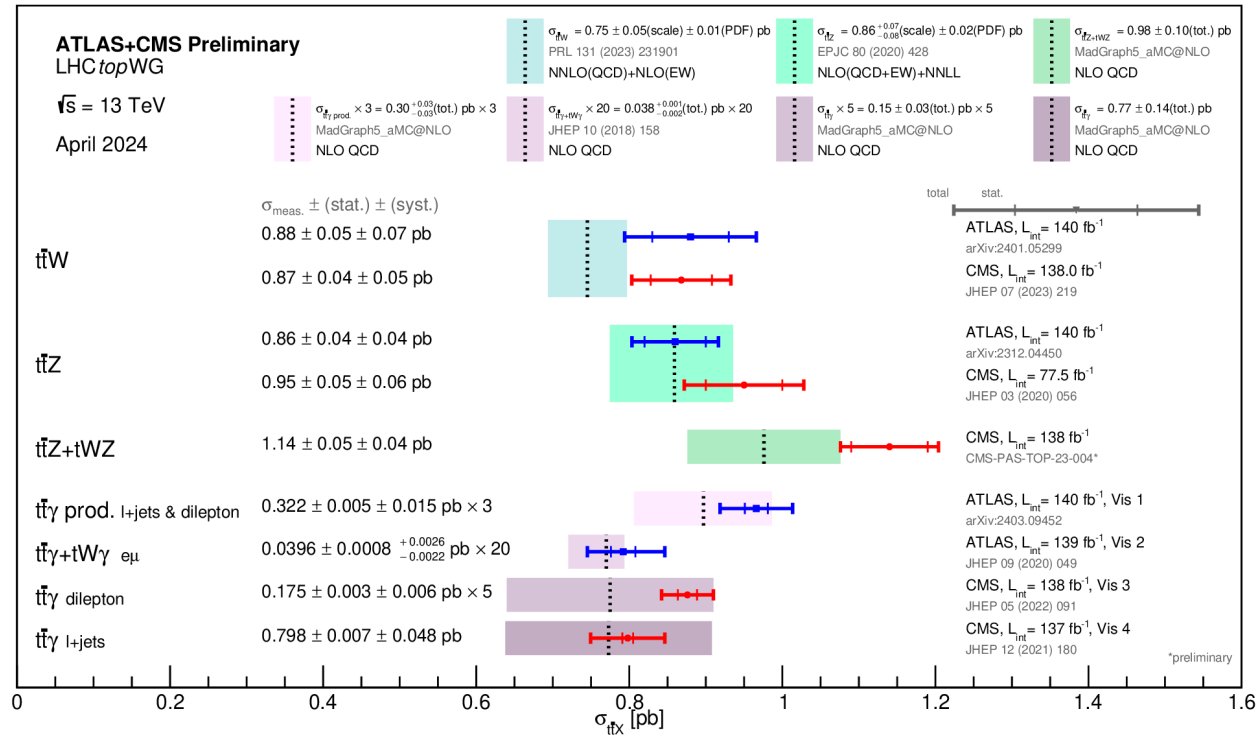


Figure 11: Expected fractional contributions of the statistical (orange) and systematic (blue) uncertainties to the total uncertainty in the measurements of the parameters of the rotated basis c' with the SMEFT linearised model (top panel), and the corresponding expected fractional contributions of experimental (cyan), signal theory (light blue) and background theory (dark blue) uncertainties to the total systematic uncertainty (bottom panel).

top + X combinations

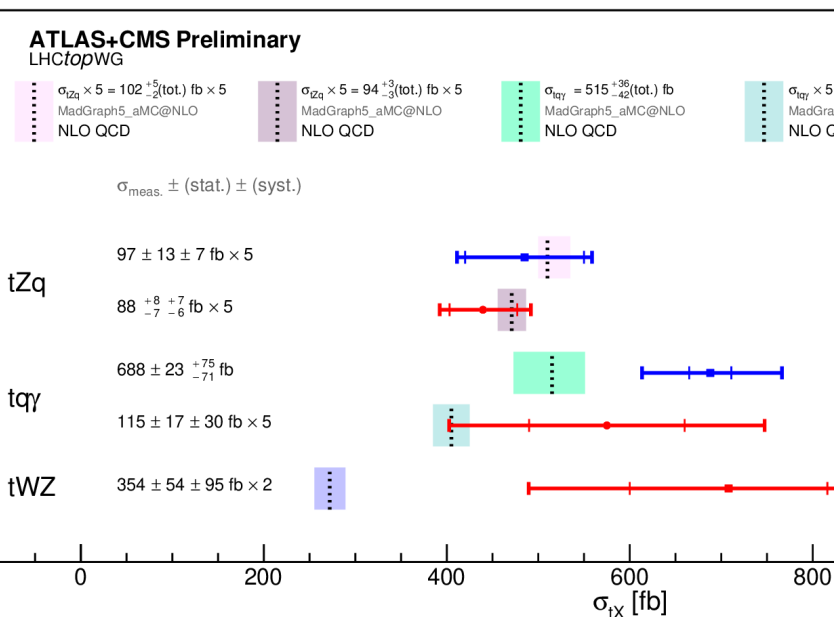
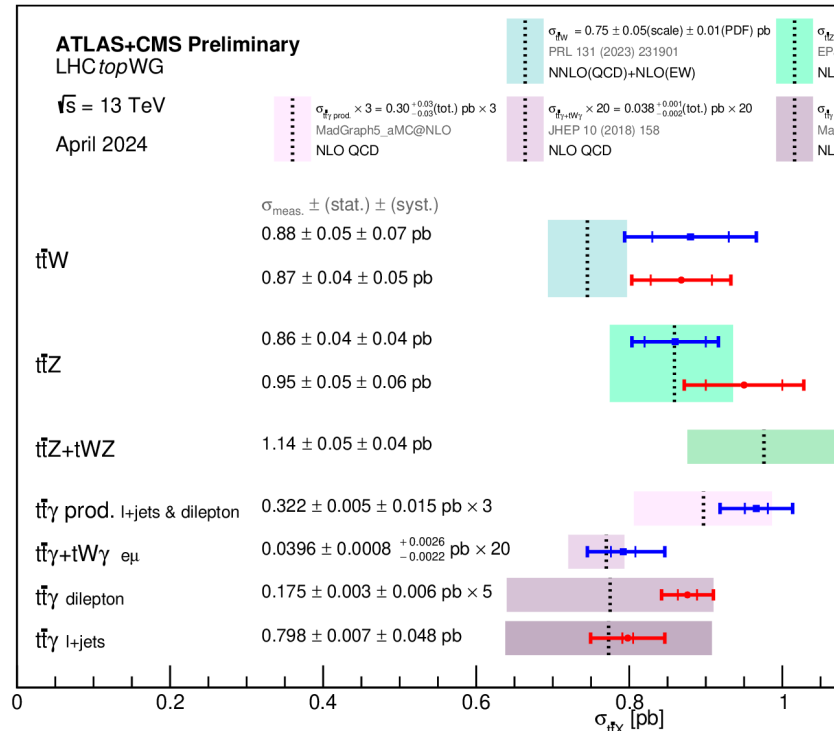
- Many top + X results



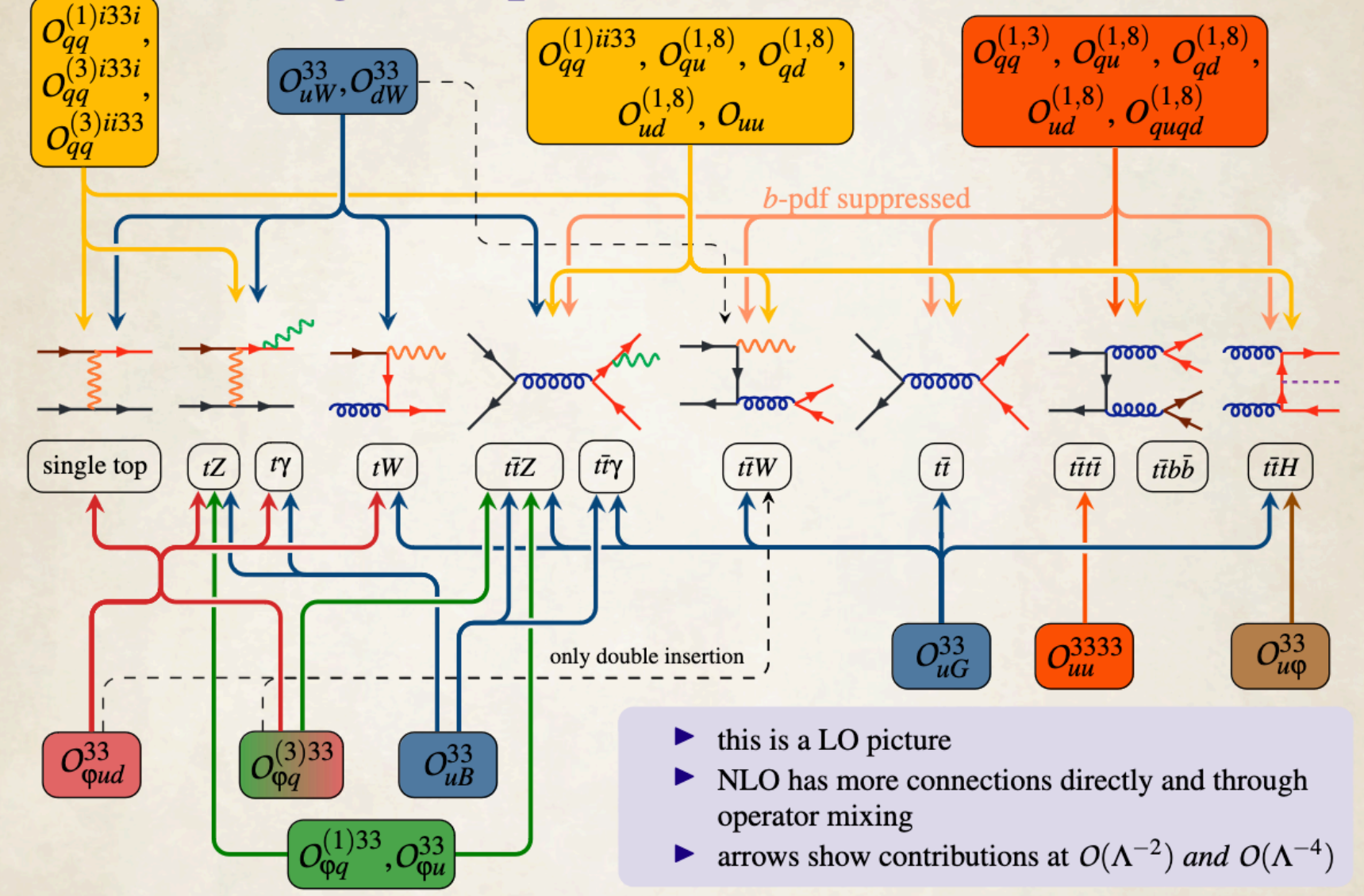
top + X combinations

- Many top + X results

- With large EFT interplay



Top EFT: a global picture

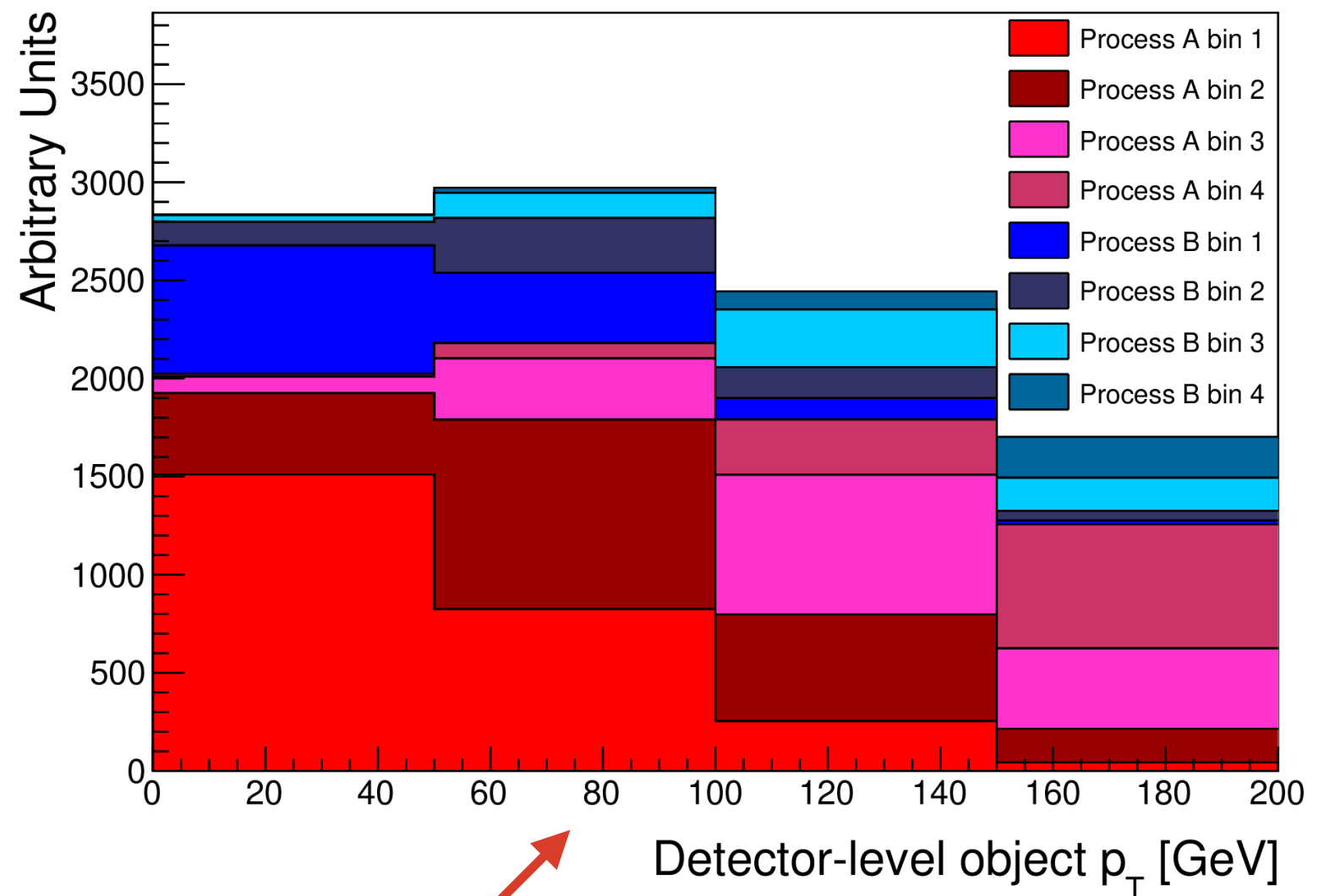


P. Galler

top + X combinations

- Similar final states in different processes (e.g 2L or 3L in ttH and ttW). Needs careful harmonisation of object definition and phase-space regions.

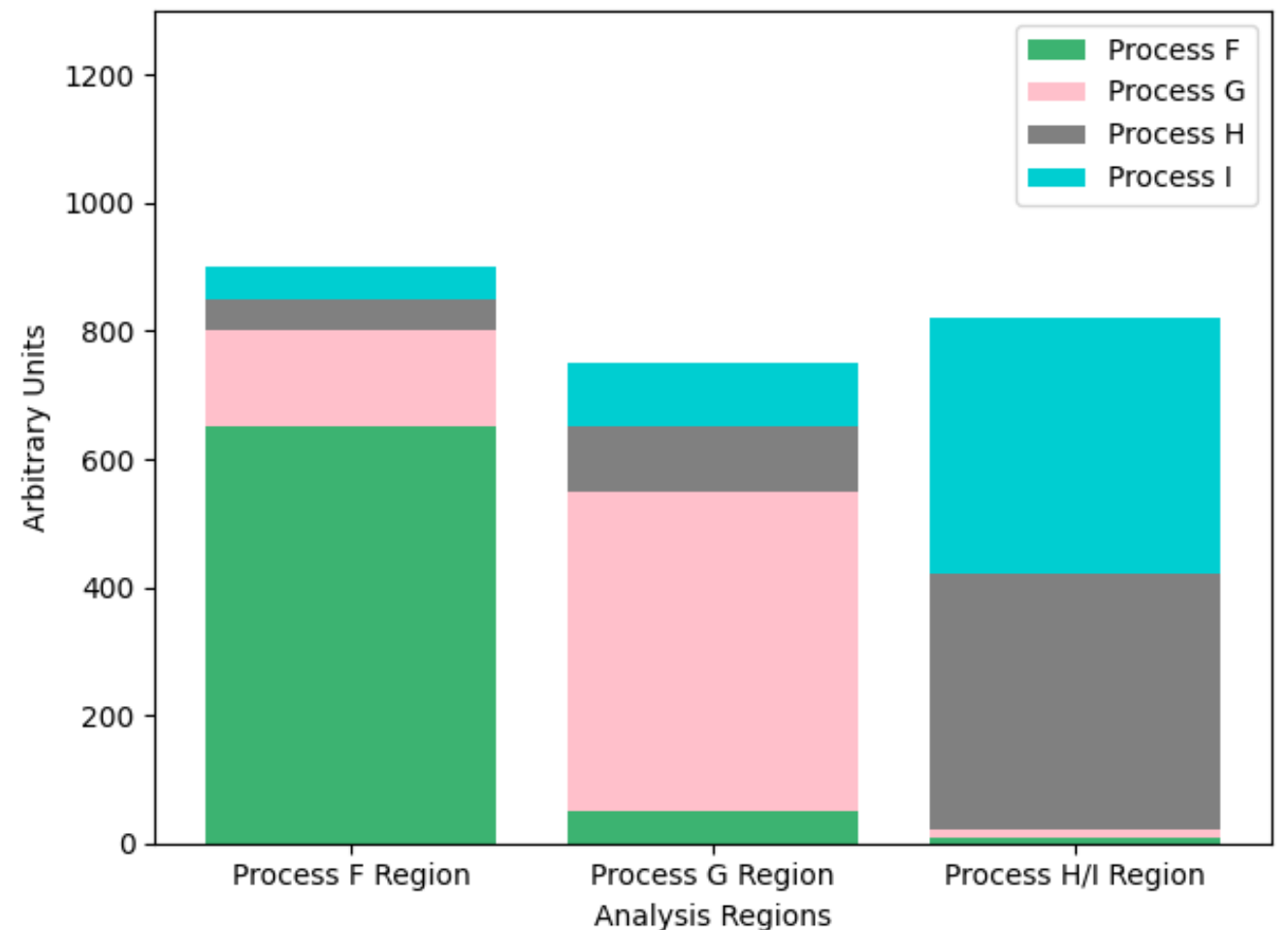
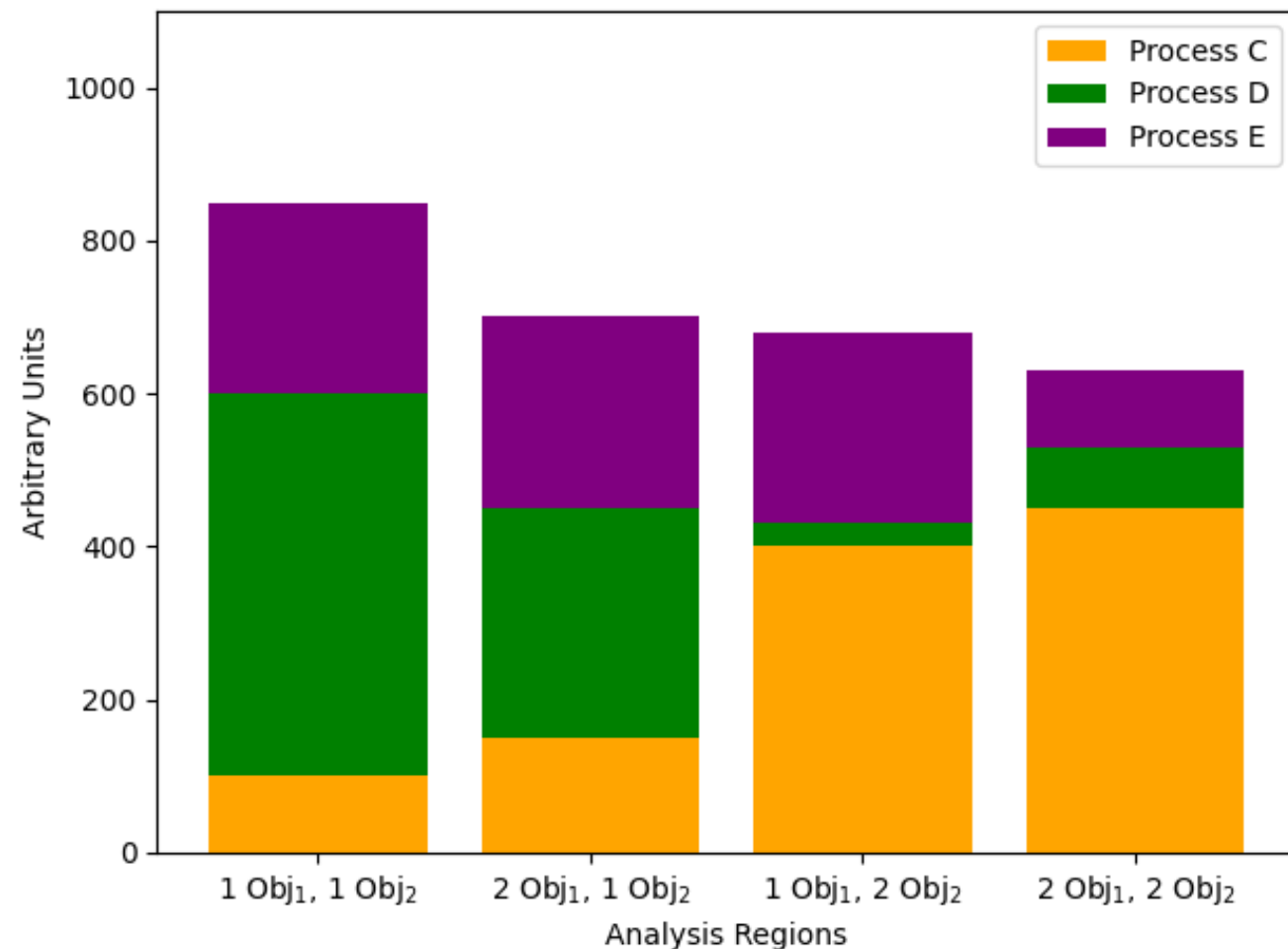
- Detector-level EFT interpretations: simple approach, but difficult reinterpretation.
- Unfolded measurements: simpler reinterpretation, but EFT effects on the background are not considered



Except in multisignal unfolding

Top + X combination

- Harmonisation of objects: correlation of uncertainties
 - ➔ e.g. ATLAS to improve prompt-lepton tagger
- Harmonisation of phase-space definitions: removal of statistical overlaps
 - ➔ Veto regions when overlap is significant
 - ➔ e.g. removal of hadronic-taus in light-lepton ttZ analysis



Top + X next-steps

Step	Stat. Overlap	Analysis overlap	EFT sensitivity overlap	Example
1	Small or 0	Largely independent	Some	ttZ and tt γ
2	Small	Overlap	Some	ttZ and ttW+j EW
3	Large	Overlap	Overlap	ttZ and tZq
4	Large	Large	Overlap	ttW, ttH and ttt
5	Large	Large	Large	As many top+X processes available

tt+X interpretations from CMS in the multi-lepton channel